

# Operation of polymer electrolyte membrane fuel cells with dry feeds: Design and operating strategies

Warren H.J. Hogarth<sup>a,b</sup>, Jay B. Benziger<sup>a,\*</sup>

<sup>a</sup> Department of Chemical Engineering, Princeton University, Princeton, NJ 08544, USA

<sup>b</sup> ARC Centre for Functional Nanomaterials, School of Engineering, The University of Queensland, Brisbane 4072, Australia

Received 21 October 2005; received in revised form 18 November 2005; accepted 23 November 2005

Available online 18 January 2006

## Abstract

The operation of polymer electrolyte membrane fuel cells (PEMFCs) with dry feeds has been examined with different fuel cell flow channel designs as functions of pressure, temperature and flow rate. Auto-humidified (or self-humidifying) PEMFC operation is improved at higher pressures and low gas velocities where axial dispersion enhances “back-mixing” of the product water with the dry feed. We demonstrate auto-humidified operation of the channel-less, self-draining fuel cell, based on a stirred tank reactor; data is presented showing auto-humidified operation from 25 to 115 °C at 1 and 3 atm. Design and operating requirements are derived for the auto-humidified operation of the channel-less, self-draining fuel cell. The auto-humidified self-draining fuel cell outperforms a fully humidified serpentine flow channel fuel cell at high current densities. The new design offers substantial benefits for simplicity of operation and control including: the ability to self-drain reducing flooding, the ability to uniformly disperse water removing current gradients and the ability to operate on dry feeds eliminating the need for humidifiers. Additionally, the design lends itself well to a modular design concept.

© 2005 Elsevier B.V. All rights reserved.

**Keywords:** PEM fuel cell; Water management; Auto-humidification; Stirred tank reactor (STR); Flow channel

## 1. Introduction

Polymer electrolyte membrane (PEM) fuel cells are increasingly being cited by governments as a possible pathway to the reduction of greenhouse gas emissions [1]. Unfortunately, there are significant barriers to commercialization including: improving the PEM operating temperature range, reducing catalyst loading, reducing balance of plant and costs [2,3]. The operation of PEMFCs at reduced relative humidity is a crucial improvement needed to reduce the balance of plant and increase the operating range of fuel cells. Nafion has been the most successful proton conductor for PEMFCs, but it must be nearly fully humidified to function effectively. Using conventional serpentine flow channel fuel cell reactors the feeds must be humidified to keep the fuel cell operational. Most approaches to solve the problem of operation with reduced feed humidification have focused on creating new proton conducting materials that conduct protons

but do not require or have a reduced dependency on water [4–7]. Other approaches have investigated changes to the flow channels in the PEM and to the operation parameters (such as flow rates, etc.); however, all these investigations are still based on a serpentine or channel flow reactors [8–11].

There are a few studies in literature that consider reduced humidity operation of serpentine fuel cells [12–16]. These studies focused on the effect of the water diffusion in the membrane and electro-osmotic drag under different performance criteria. These studies demonstrated that under a range of conditions cathode reactant water could partially humidify the membrane. The general conclusions were that water transport from the cathode to the anode was highest at low currents, and in all cases some humidification was required. These studies all employed feed flows in excess of stoichiometric to prevent liquid water forming in the system and creating flooding problems. Unfortunately high flow rates with dry feeds tend to dry the membrane by sweeping water out of the fuel cell.

These previous studies were restricted to serpentine flow channel systems. The compromise with serpentine systems is that high flow rates are required to prevent liquid blockage of

\* Corresponding author. Tel.: +1 609 258 5416; fax: +1 609 258 0211.  
E-mail address: [benziger@princeton.edu](mailto:benziger@princeton.edu) (J.B. Benziger).

### Nomenclature

$A_{\text{channel}}$	cross-sectional area of gas flow channel
$D$	gas phase water diffusivity
$F$	Faraday's constant
$F_A$	molar flow rate at the anode
$F_C$	molar flow rate at the cathode
$i$	current
$j$	current density
$P_T$	total pressure
$P_w$	partial pressure of water
$P_w^0$	vapor pressure of water at cell temperature
$t$	time
$x$	stoichiometric excess of feed flow rates
$z$	axial position along flow channel

the flow channels. When operating with reduced humidities in serpentine flow channels concentration and current gradients exist along the channels. The observed currents are an average of the conditions along the length of the flow channel.

Our research group has reengineered the PEMFC fuel delivery system to utilize the water created at the cathode to humidify both reaction chambers. In doing so we have considered the anode and cathode chambers of the fuel cell as individual reactors and applied reactor design heuristics to solve the hydration problem. This approach has also enabled us to simplify the analysis of fuel cell operation [17–20]. By redesigning the fuel delivery system we have been able to replicate fully humidified operation of a PEMFC with dry feed. We have exploited gravity to facilitate liquid water removal in the channel-less self-

draining PEM fuel cell; this novel design removed the need to have high flow rates by promoting the back-mixing of the dry feed gases with the humidified reactant gases in the fuel cell.

To understand the basic water management in PEMFCs it is necessary to consider what happens to the water that is produced at the cathode? One of the common problems experienced operating PEMFCs at high currents is mass transfer limitations in the GDL caused in part by having too much water present [21]. The excess of water causes blockages of the flow channels [22] and flooding in the catalyst layer of the GDL. Such phenomena limit the operating range of the fuel cell and hence will hinder its ability to effectively control power output. To better utilize the water produced at the cathode and improve robustness of operation, the water balance should be optimized. That is, a balance must be struck between reactant gases transported from the gas flow channel to the electrode/membrane interface, and the amount of water that is transported away from the electrode/membrane interface (Fig. 1). The mechanisms for this process have been investigated in recent papers [21,23]. The PEMFC should be operated under conditions where liquid water does not hinder gas transport to the electrode/electrolyte interface. In our previous studies of water flow in the GDL we found that water will normally be excluded from the hydrophobic GDL [21]. Only when a hydrostatic pressure is applied to push water into the GDL will liquid water accumulate in the GDL. Liquid water will accumulate in the gas flow channels outside of the GDL. In a conventional serpentine flow channel PEM fuel cell the gas velocity must be sufficient to push the liquid water through the flow channels. We developed the free-draining design to permit liquid water to flow gravity in an open plenum.

To achieve optimal water balance the water produced in the fuel cell should precisely match the water removed in the

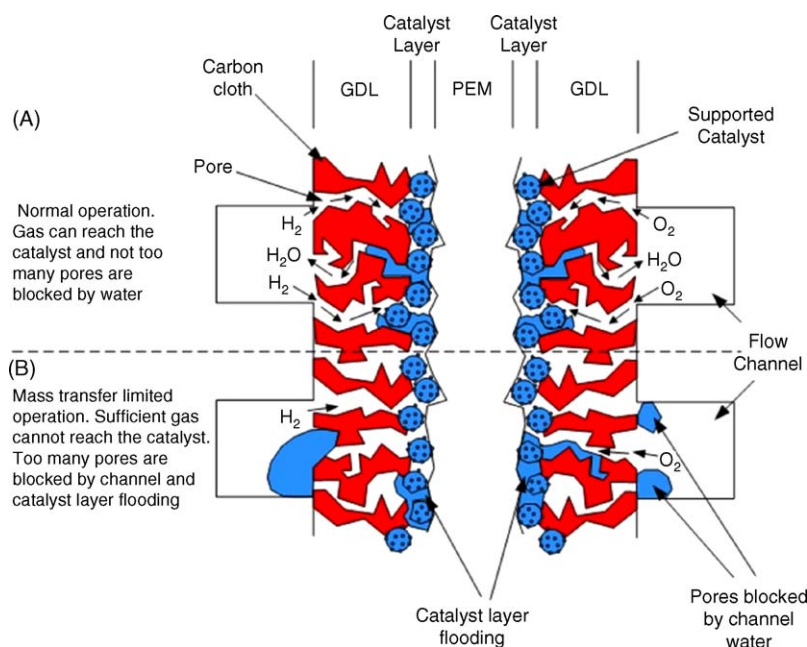


Fig. 1. Mass transport processes in the gas diffusion layer of a PEMFC. (A) Under normal operation (ohmic region) enough gas can penetrate the gas diffusion layer (GDL) to reach the catalyst and water is effectively removed. (B) At high currents, more water is produced causing two pore blocking effects: flooding of the catalyst layer and channel blockage due to water condensation in the flow channels. Blockage of the flow channels can be influenced by flow channel design.

effluents from the fuel cell. Methods of running a fuel cell at reduced humidities often overlook this internal production of water and focus exclusively on the feed RH, upstream of the fuel cell. Generally the RH of the feed is not measured directly, rather the temperature of the humidifier bottle is reported. The RH of the feed may vary substantially depending on the flow rate and gas dispersion efficiency of the humidifier. Additionally, flow rates for fuel cell experiments are often set very high to avoid build up of liquid water in the flow channels. High flow rates in a fuel cell lead to a very low single pass conversion (low fuel utilization).

A holistic approach to this problem is to consider what happens with the water that is produced internally in the fuel cell. In our laboratory this commenced with an investigation of what happens to the water that is produced within the fuel cell; how much is produced, where does this exit the cell (anode or cathode), what is the effect of changing the flow rates, temperature and pressure? We then ask how can one use the information about the water balance to our advantage for fuel cell design? The investigation posed the question: “*if one of the significant problems with fuel cell operation is having too much water and the fuel cell is a net producer of water, why is more water added to the cell?*” We have investigated the effect and consequences of the water balance in a fuel cell elsewhere [24,25]. Here we report on how understanding the water balance in the fuel led us to rethink the way that the flow channels of a fuel cell are designed.

## 2. Experimental

Experiments were conducted on two different designs of gas flow systems in PEM fuel cells. Both fuel cells used the same construction of membrane-electrode-assembly (MEA). One fuel cell design was custom built to behave as coupled stirred tank reactors (STR) (Fig. 2A). In the STR design the flow channels are replaced with an open plenum and distributed pillars to apply uniform pressure to the MEA. The MEA in the STR fuel cell had a nominal electrode/electrolyte area  $1.9 \text{ cm}^2$ . Results with the

STR fuel cell were compared to those obtained with a commercially available Globetech fuel cell test station with serpentine flow channels (Fig. 2B). The Globetech test station had MEAs with nominal electrode/electrolyte area  $5 \text{ cm}^2$ .

The STR fuel cell was run auto-humidified; dry feeds of  $\text{H}_2$  and  $\text{O}_2$  were fed to the anode and cathode, respectively (auto-humidified mode) through mass flow controllers. Details of the construction and operation are reported elsewhere [24,25]. The effluents were connected to spring loaded check valves with adjustable cracking pressures (Swagelok SS-4CPA2-3). The check valves were adjusted to permit the system to run pressurized between 1 and 3 bar. The fuel cell was positioned between aluminum blocks and temperature controlled by cartridge heaters; the schematic of the system is shown in Fig. 3.

The Globetech test station (Globetech Inc., GT-1000) was equipped for the temperature-controlled humidification of the reactant gases ( $\text{H}_2$ ,  $\text{O}_2$ ) and for the temperature control of the single cell. Flow rates of the gases were regulated using mass-flow controllers. The total pressure of the gases was controlled using back-pressure regulators. The cell was fed with humidified  $\text{H}_2$  and  $\text{O}_2$  at 1 or 3 bar (reactant gas and water vapor pressure equal to 1 or 3 bar) and the temperature of the  $\text{H}_2$  and  $\text{O}_2$  humidifiers and of the single cell were 90 and 80 °C, respectively. After the single cell had reached stable conditions cell potential versus current measurements were then made under the desired conditions of temperature and pressure in the PEMFC. Identical procedures were followed for all of the membranes.

Because the STR PEM fuel cell and the Globetech test station had different size MEA we operated at the same normalized flow rate, so water production or fuel consumption per unit area could be directly compared for the two fuel cells. The feed flow rates for both the Globetech and STR fuel cells at 3 atm were 9 and 4.5 sccm  $\text{cm}^{-2}$  for  $\text{H}_2$  and  $\text{O}_2$  respectively for dry feed experiments. At 1 atm the flow rates were 5 and 2.5 sccm  $\text{cm}^{-2}$  for  $\text{H}_2$  and  $\text{O}_2$ , respectively. These flow rates were  $\sim 10\%$  stoichiometric excess of the maximum currents obtained with the fuel cell ( $\sim 1.1 \text{ A cm}^{-2}$  at 3 atm and  $\sim 0.6 \text{ A cm}^{-2}$  at 1 atm). The feed flow rates for  $\text{H}_2$  and  $\text{O}_2$  in the humidified experiments were

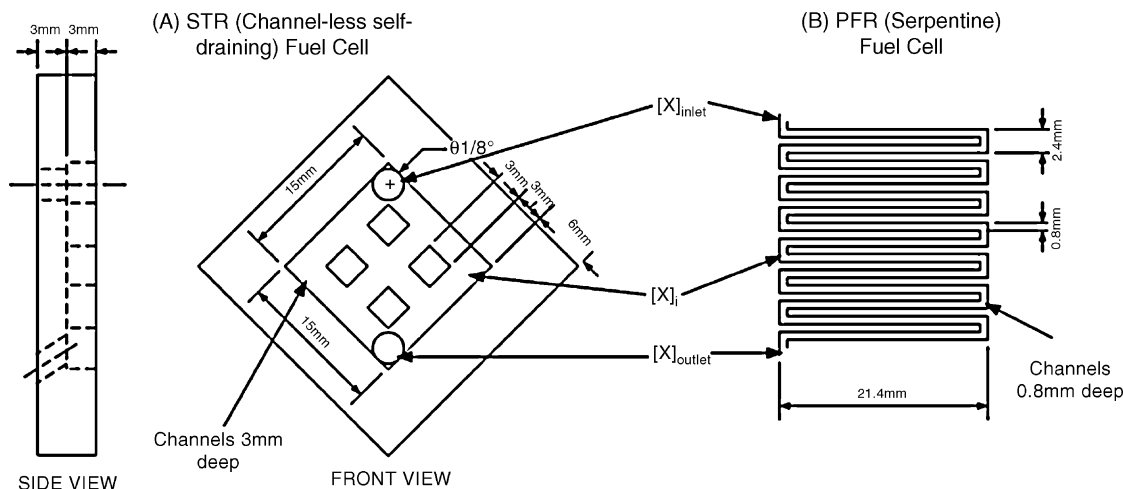


Fig. 2. Fuel cell flow channel design. (A) A side and profile view of the channel-less self-draining STR fuel cell electrodes. (B) The serpentine flow channel design of the electrode plate for the Globetech fuel cell test station.

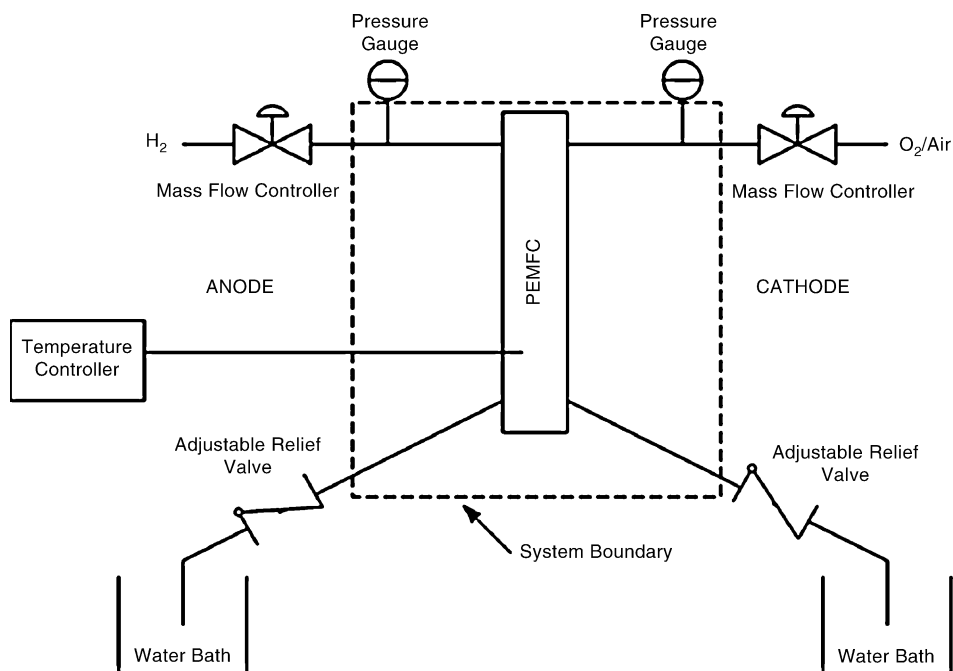


Fig. 3. Schematic of the fuel cell system. The feed gases were metered in through mass flow controllers. The pressure was fixed by adjustable relief valves on the outlets of the fuel cell. The cracking pressure on the relief valves was set to keep the desired cell pressure.

20 and 10 sccm  $\text{cm}^{-2}$  respectively,  $\sim 2.5$  times stoichiometric at maximum current. We chose to run the fuel cells with fixed flow rates, and did not vary the flow rate with the fuel cell current as is sometimes done. In other experiments (not reported here), we found that feedback control that slaved the reactant feed to the current can lead to instabilities [26,27]. To avoid the complexities of non-linear system responses from the control systems we found it better to run the experiments with fixed flow rates. This is particularly true when operating with dry feeds where changes to the flow rates alter the water content in the membrane, which feeds back to the water production rate.

The same membrane electrode assemblies (MEAs) were used in both fuel cells. MEAs were prepared using Nafion 115 membranes (Ion Power Inc., Bear, DE). These were sequentially boiled in DI water, 3% hydrogen peroxide, DI water and 1 M sulfuric acid solutions respectively to remove impurities. The membranes were sandwiched between two ELAT style electrodes (E-tek Division of DeNora, Somerset, NJ) with 10 wt.% Pt catalyst on carbon. Electrodes were painted with  $0.6 \text{ mg cm}^{-2}$  of Nafion prior to being pressed at  $140^\circ\text{C}$  for 90 s at 40 MPa.

Fuel cell  $I$ - $V$  data was obtained on an Arbin Instruments MSTAT4+ test station. All tests were equilibrated until steady state was achieved prior to sweeping  $I$ - $V$  curves. Typically it took between 1 and 4 h to achieve steady state, sometimes it took up to 24 h for steady state to be achieved. The MEA was equilibrated at a series of fixed voltages (0.1–0.8 V) or external resistances (0.2–10  $\Omega$ ) at each individual temperature before sweeping the  $I$ - $V$  curves at  $20 \text{ mV s}^{-1}$ . The sweeps were completed in  $<90 \text{ s}$  to minimize the effects of changing water content in the membrane. A current interrupt technique was used to measure the internal resistance of the MEA. The voltage response was recorded after 10 40 mA pulses were applied 1 ms apart.

The MSTAT4+ software was used to analyze the data. Tests were carried out on multiple MEAs, with each individual MEA often being tested for up to 2 weeks. We only tested the serpentine flow channel fuel cell at  $80^\circ\text{C}$ , this represented the base temperature for comparison as this has been cited by vehicle manufacturers as the highest temperature where Nafion can reliably operate [3]. We compare this base case to operation of the STR fuel cell at temperatures from 25 to  $115^\circ\text{C}$ .

### 3. Results

The aim of the work was to demonstrate dry feed performance of a PEMFC and to elucidate the role of flow channel design. The well mixed condition in the STR design is achieved by having the residence time for flow through the gas chambers be long compared to the time for gaseous diffusion in the chambers ( $\tau_{\text{residence}} = V/Q$ ,  $\tau_{\text{diffusion}} = V^{2/3}/D$ ). The experiments reported here compare and contrast design options (channel-less versus serpentine flow channels) and demonstrate under which conditions each is likely to operate optimally.

The primary concern when using Nafion polymer membranes (and other water reliant membranes) is that the membrane be sufficiently hydrated to permit good proton conductivity. Membrane resistance is directly related to the activity of water (relative humidity) in the flow channels [28]. Water activity is the ratio of the partial pressure of water to the vapor pressure at the cell temperature. With the STR design the composition is uniform across the MEA at each electrode. We measured the relative humidity of the effluent streams as this provides us with a direct measure of the water activity at each electrode.

Fig. 4 compares the operation of PEMFCs with dry feeds to a serpentine flow channel fuel cell with fully humidified feeds.

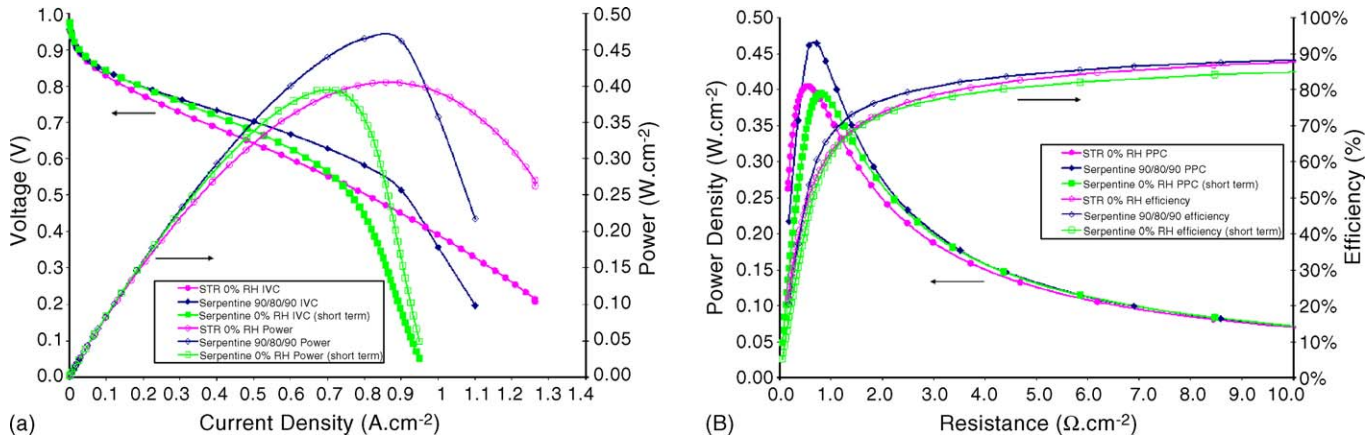


Fig. 4. Direct comparison of the performance data for the channel-less self-draining STR fuel cell to a standard commercially available serpentine flow channel design (Globetech). The STR cell is operating on bone dry feeds at 80 °C and 3 atm while the serpentine cell was operated at the same conditions with both dry and fully humidified streams (90/80/90 anode/cell/cathode). (a) Shows the polarization curves and power density (over the external load) as a function of the current density. (b) Shows the power performance curve (PPC) and efficiency as a function of the external load impedance.

The fuel cells were operated at 80 °C at 3 bar pressure. The feed streams for the humidified fuel cell were bubbled through humidifiers at 90 °C, it is assumed that those gas streams are fully humidified at the fuel cell temperature of 80 °C. The fuel cells operated with dry feeds were equilibrated at voltages of 500 mV for 4 h before taking the *i*-*v* data. Similar results were obtained when the cells were equilibrated at 200–700 mV. When the serpentine flow channel fuel cell was equilibrated above 800 mV for more than 30 min the current extinguished. The STR fuel cell could be equilibrated up to 850 mV before extinguishing the current. Additionally liquid water could be seen exiting the dry feed cells at the anode and the cathode when equilibrated at a voltage up to 700 mV.

Fig. 4a shows the *j*-*v* curves for the three fuel cell operations, also shown is the power density as a function of current density. Fig. 4b shows the power performance and fuel efficiency curves for the three fuel cells. The power performance is the power density as a function of the load resistance normalized to the MEA area. Efficiency is the fraction of energy produced by the fuel cell that is dissipated in the load resistance (*V*/*V*<sub>0</sub>).

The results in Fig. 4a suggest that at current densities below 0.7 A cm<sup>-2</sup> (0.6 V) there is little difference in operation between the humidified fuel cell and the fuel cells operating with dry feeds. The serpentine flow channel fuel cell with dry feeds shows the on-set of mass transfer limitations at the lowest current density of ~0.8 A cm<sup>-2</sup>. The humidified serpentine fuel cell showed the high power density of 0.95 W cm<sup>-2</sup> at a current density of ~0.85 A cm<sup>-2</sup>, above that current density the voltage and power density both decreased rapidly. The STR fuel cell with dry feeds showed that it provided higher voltage and greater power densities at high current densities than a serpentine flow channel fuel cell operating with either humidified feeds or dry feeds. These results suggest that the STR design delays the on-set of mass transfer limitations.

Fig. 4 is somewhat deceiving when looking at the results with dry feeds. This is because the dry feed performance of a fuel cell is a function of the water produced by the current. The design can have an influence on how this water is distributed. Hence, because the *j*-*v* data is swept out over a short period of time (90 s) the data reflects the performance of the cell at the water

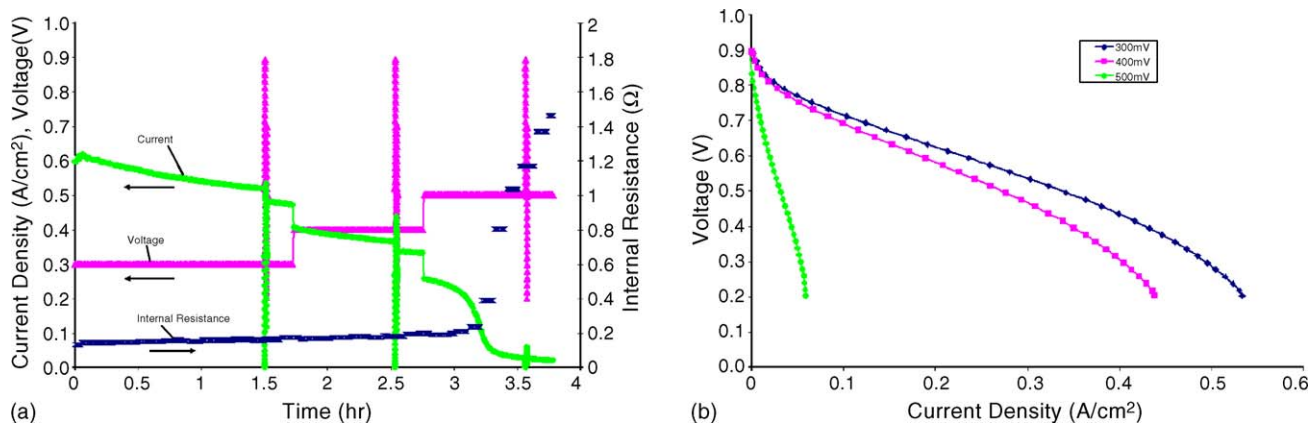


Fig. 5. (a) Chronological data of current, voltage and internal resistance of a serpentine flow channel fuel cell operated at 80 °C and 1 bar with dry feeds. The cell was pre-conditioned for 4 h under voltage control at 200 mV. The cell was operated under voltage control. For 0–1.7 h, *V* = 300 mV; 1.7–2.7 h, *V* = 400 mV; 2.7–3.7 h, *V* = 500 mV. The spikes on the current trace correspond to *i*-*v* scans. (b) The *j*-*v* curves at 300, 400 and 500 mV.

content corresponding to the current at which it was equilibrated under. If the fuel cell were equilibrated with a large voltage of >850 mV (corresponding to a low current density) the  $j-v$  curve has a much different appearance than shown in Fig. 4. The MEA resistance increases dramatically over time as the fuel cell dries out due to the low current. At the other extreme, equilibrating the fuel cell at low voltages causes liquid water buildup in the fuel cell reducing the maximum current density [25]. When the equilibration voltage of the serpentine fuel cell was reduced from 500 to <200 mV, the maximum current density that was obtained in a  $j-v$  sweep is reduced from 0.95 to 0.75 A cm<sup>-2</sup>. There was minimal performance reduction at low voltage and high currents with the STR fuel cell.

The time for equilibration and its effects are illustrated in Fig. 5 for the serpentine fuel cell operated at 80 °C and 1 bar pressure. The fuel cell was operated under voltage control and the current, voltage and MEA resistance are plotted as functions of time. The voltage was stepped at different time intervals; the load resistance was controlled to maintain the voltage, the current through the load resistance and the internal MEA resistance were recorded as a function of time. From time = 0 to 1.7 h the voltage set-point was 300 mV. The MEA resistance was constant, while the current decreased over time indicating liquid water was restricting the total current. When the voltage was stepped to 400 mV at just after 1.7 h, the same behavior was observed. When the voltage was stepped to 500 mV after 2.7 h there was a 0.25 h lag and then the current dropped and the MEA resistance increased suggesting that insufficient water was being produced to keep the membrane hydrated. The  $j-v$  curves presented in Fig. 5b reflect this behavior. There was a slight decrease in performance between 300 and 400 mV. At 500 mV the performance was significantly worse with a lower open-circuit voltage and steep slope, both suggesting the membrane had now dried.

Fig. 6 shows a similar chronological history of the STR PEM fuel cell operation at 1 bar and 80 °C. We have also recorded the relative humidity at the anode and cathode. The results are similar to those with the fuel cell with serpentine flow channels, however the current is more stable. The current changed with

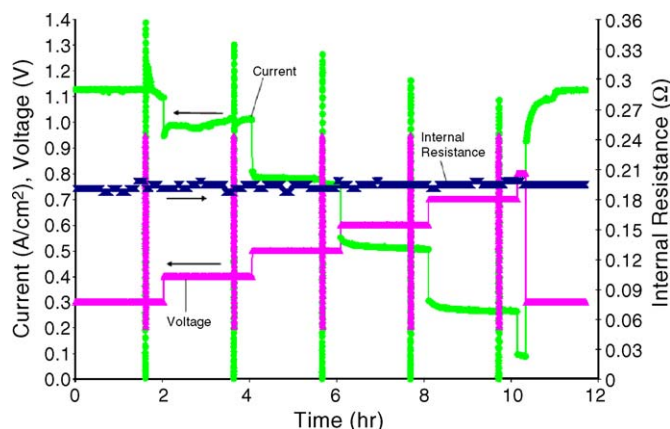


Fig. 7. Chronological data of current, voltage and internal resistance of an STR fuel cell operated at 80 °C and 3 bar with dry feeds. The cell was pre-conditioned for 4 h under voltage control at 200 mV. The cell was operated under voltage control at the set-points as shown. The spikes on the current trace correspond to  $i-v$  scans.

each voltage step and was nearly constant at all voltages up to 450 mV and current densities of 240 mA cm<sup>-2</sup>. When the voltage was increased to 500 mV the current decreased over time, while the internal resistance of the MEA increased. The relative humidities at the anode and cathode were near 100% for voltages controlled at <450 mV, but when the voltage was increased to 500 mV the relative humidities declined. For a more detailed analysis of the RH response of the system refer to Ref. [25]. The current, internal resistance and relative humidity results all show that at voltages >500 mV the current density was insufficient to keep the membrane hydrated. At these higher voltages and lower current densities the auto-humidified fuel cell extinguished with the current density approaching zero.

Fig. 7 presents the chronological history of the auto-humidified STR PEM fuel cell operation at 80 °C and 3 bar. The STR fuel cell operates to high voltages and lower currents that the serpentine flow channel fuel cell before the current is extinguished. The voltage was run up to 800 mV and a current density of 90 mA cm<sup>-2</sup> without extinguishing. By increasing the

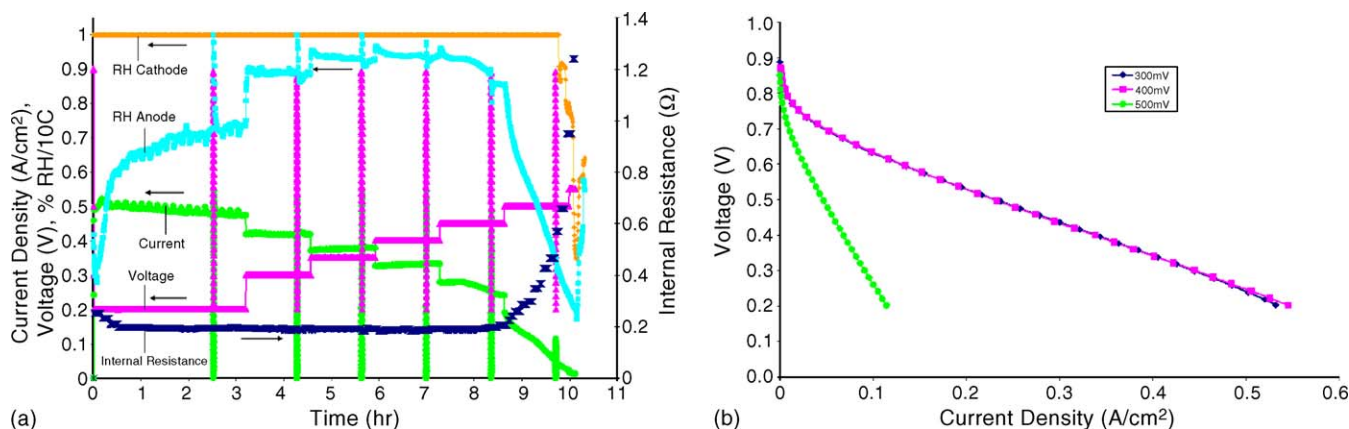


Fig. 6. (a) Chronological data of current, voltage and internal resistance, RH anode and RH cathode of an STR fuel cell operated at 80 °C and 1 bar with dry feeds. The cell was pre-conditioned for 4 h under voltage control at 200 mV. The cell was operated under voltage control. For 0–3.2 h,  $V=200$  mV; 3.2–4.6 h,  $V=300$  mV; 4.6–6.0 h,  $V=350$  mV; 6.0–7.3 h,  $V=400$  mV; 7.3–8.6 h,  $V=450$  mV; 8.6–10 h,  $V=500$  mV. The spikes on the current trace correspond to  $i-v$  scans. (b) The  $j-v$  curves at 300, 400 and 500 mV.

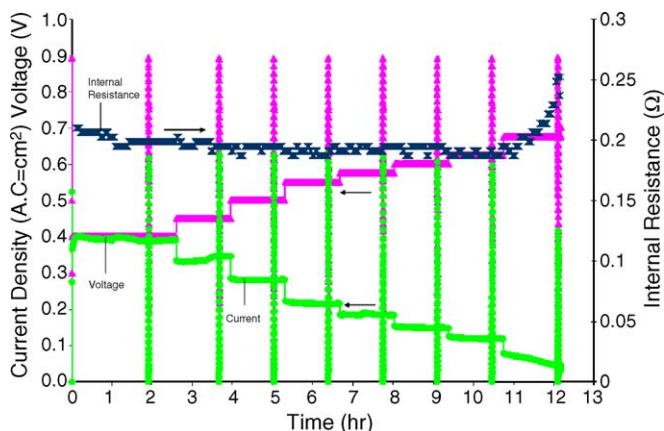


Fig. 8. Chronological data of current, voltage and internal resistance of an STR fuel cell operated at 60 °C and 1 bar with dry feeds. The cell was pre-conditioned for 4 h under voltage control at 200 mV. The cell was operated under voltage control as shown.

pressure the fuel cell was able to operate to higher temperatures without extinguishing, even though the flow rates were now in considerable excess.

Figs. 8 and 9 present chronological histories of the auto-humidified STR PEM fuel cell operating at 60 °C and 1 bar and 95 °C and 3 bar, respectively. By reducing the temperature from 80° to 60° at 1 bar the fuel cell could be operated auto-humidified at voltages up to 625 mV and currents down to 120 mA cm<sup>-2</sup> without extinguishing. The extinguishing current density at 60 °C was half that at 80 °C. In contrast increasing the temperature at 3 bar from 80° to 95° caused the extinguishing current density to increase.

Fig. 10 compares the  $j$ - $v$  curves for STR PEM fuel cells operating at 3 bar and temperatures from 25° to 115° (equal flow rates). These were all obtained after equilibrating the fuel cell with a fixed external load of 1 Ω, except for the 115 °C data where equilibration was done with a 0.2 Ω load. The current density at fixed voltage increases with temperature from 25 to 95 °C and then decreases as the temperature is increased to 115 °C. The relative humidity at the anode and cathode both decreased to

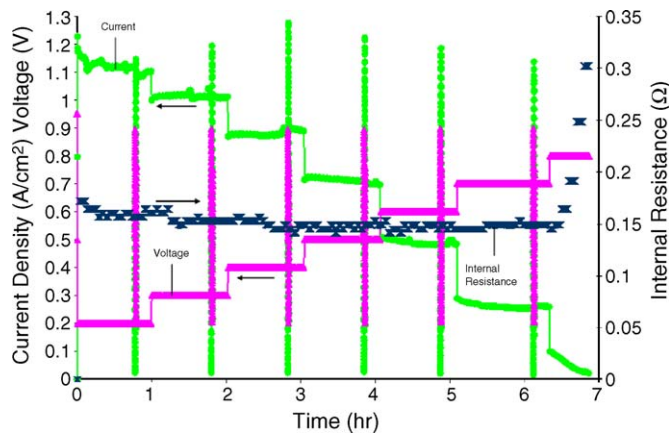


Fig. 9. Chronological data of current, voltage and internal resistance of an STR fuel cell operated at 95 °C and 3 bar with dry feeds. The cell was pre-conditioned for 4 h under voltage control at 200 mV. The cell was operated under voltage control.

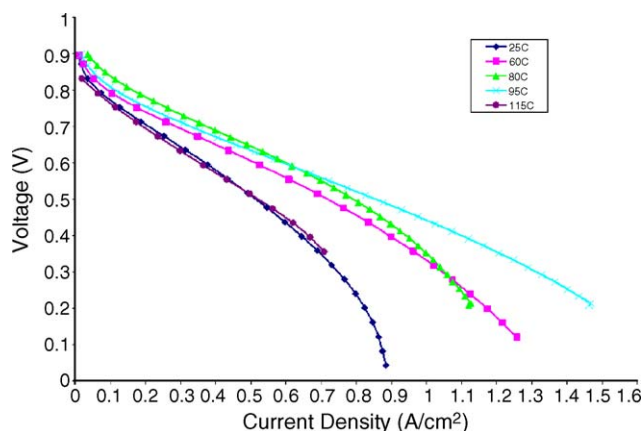


Fig. 10. Temperature effect on the  $j$ - $v$  performance of the STR fuel cell. The  $j$ - $v$  curves were swept after equilibrating the fuel cell for at least 1 h with an external load of 1 Ω, except for the 115 °C which was equilibrated with a 0.2 Ω load. Feed flow rates of 10 and 5 sccm H<sub>2</sub>/O<sub>2</sub> were used for all experiments.

<100% at 115 °C indicating that the fuel cell was drying out. The  $j$ - $v$  curves for the STR fuel cell operating above 60 °C do not show any region of strong mass transfer limitations. Even though there is liquid water present the free draining by gravity keeps the liquid from inhibiting mass transfer to the electrode/electrolyte interface.

#### 4. Discussion

The key results may be summarized:

1. PEM fuel cells can operate auto-humidified with dry feeds above 100 °C.
2. PEM fuel cells dry out and the current extinguishes if the voltage drop across the load is too high, and the current is too low.
3. Increasing the pressure improves auto-humidification operation and is essential to operation above 100 °C.
4. Flow field design effects extinguishing current and voltage.
5. Flow field design can significant reduce mass transfer at high current.

The operation of PEM fuel cells with dry feeds can greatly simplify the operation and control of the overall fuel cell system. We have operated auto-humidified STR PEM fuel cells for periods of 2–3 months with no maintenance or control. The simplicity of auto-humidification would be a tremendous benefit for commercial applications of PEM fuel cells. However, a PEM fuel cell will only operate with auto-humidification in certain parameter space of temperature, pressure, flow rates, current, voltage and load resistance. We wish to identify the critical operating parameters for PEM fuel cells that govern operation with dry feeds.

Auto-humidified PEM operation requires that water production in the fuel cell must equal or exceed the rate of water removal. When such a condition is met there is sufficient water to fully humidify the reactant gas streams to 100% RH. Water production is simply half the fuel cell current density. Water

removal occurs via convection and diffusion. The water balance at any position along the flow channel is given by Eq. (1)

$$\begin{aligned} \frac{d}{dz} \left[ (F_A + F_C) \frac{P_w}{P_T} + A_{\text{channel}} D \frac{P_T}{RT} \frac{d(P_w/P_w^o)}{dz} + \frac{i}{2F} \right] \\ = A_{\text{channel}} \frac{P_T}{RT} \frac{d(P_w/P_w^o)}{dz} \end{aligned} \quad (1)$$

For sustained auto-humidified operation  $dP_w/dz \geq 0$  at all positions in the fuel cell. We consider two extreme cases of flow for Eq. (1). The stirred tank reactor assumes that diffusion is infinitely fast so  $dP_w/dz = 0$  everywhere in the fuel cell. At the other extreme is where diffusion goes to zero,  $D = 0$ , and the gases move through the fuel cell flow channels with no axial mixing (along the length of the flow channel); this is the “plug flow” approximation.

#### 4.1. Stirred tank reactor fuel cell reactor

When diffusion is infinitely fast there are no gradients internal to the fuel cell. At steady state Eq. (1) can be integrated from  $P_w = 0$  at the inlet to  $P_w = P_w^o$  (the vapor pressure of water at the outlet). We chose the outlet pressure of water to be the vapor pressure because that represents the maximum convective flow of water out of the fuel cell. That is also consistent with the experimental observations that auto-humidification was only sustained when the effluent relative humidities were at or close to 100%. The result of integrating Eq. (1) is the minimum fuel cell current that will keep the fuel cell hydrated

$$\begin{aligned} \frac{i}{2F} \geq (F_A^{\text{out}} + F_C^{\text{out}}) \frac{P_w^o}{P_T}, \\ \frac{i}{2F} \geq \left( F_A^{\text{in}} + F_C^{\text{in}} - \frac{i}{4F} \right) \frac{P_w^o}{P_T} \Rightarrow \frac{i}{4F} \geq \frac{F_A^{\text{in}} + F_C^{\text{in}}}{2 + \frac{P_T}{P_w^o}} \end{aligned} \quad (2)$$

Eq. (2) is a simple statement of the requirement for auto-humidification with the STR PEM fuel cell. The minimum current to have sustained auto-humidification depends on the molar flow rate of the feeds and total pressure and water vapor pressure. Eq. (2) can be extended to set pressure requirements for auto-humidification as functions of the feed stoichiometric excess, and the temperature. We define the feed excess  $x$  as the fraction of the molar flow to maintain the current, as per Eq. (3)

$$F_A^{\text{in}} = \frac{i}{2F} (1 + x) \quad (3)$$

If the feeds are operated with  $\text{H}_2:\text{O}_2$  ratio of 2:1 the ratio of total pressure to water vapor pressure at the cell temperature is a simple function of the excess as given by Eqs. (4) and (5) for  $\text{O}_2$  and air feeds

$$\frac{P_T}{P_w^o} > 1 + 3x \quad \text{O}_2 \text{ feed} \quad (4)$$

$$\frac{P_T}{P_w^o} > 5 + 7x \quad \text{air feed} \quad (5)$$

Eqs. (4) and (5) are key results for operation with dry feeds. They set simple minimum requirements relating pressure, temperature

and stoichiometry that must be met for auto-humidification. The minimum total pressure requirement for auto-humidification is when there is no excess feed ( $x = 0$ ). With pure oxygen and hydrogen feeds the minimum total pressure for auto-humidification must be the water vapor pressure at the cell temperature. Operating a PEM fuel cell at 1 bar sets the maximum water vapor pressure at 1 bar. By increasing the total pressure of the fuel cell to 3 bar the maximum temperature for auto-humidification is increased to 133 °C. The increase in temperature for auto-humidified operation was verified by the experimental results; auto-humidified operation could be sustained at a current density of 90 mA cm<sup>-2</sup> at 3 bar and 80 °C, but the fuel cell would extinguish if the pressure was reduced to 1 bar at the same temperature and current density.

The maximum temperature for auto-humidification is substantially reduced for operation with air. The ratio of the total pressure to the water vapor pressure must be greater than 5 to operate auto-humidified. At 1 bar total pressure the fuel cell temperature must be below 55 °C for auto-humidified operation with air. At first glance it may be surprising that total pressure is a key parameter for auto-humidified operation. Total pressure alters the balance between total molar flux and water flux. Water vapor convection is independent of the total pressure, it is determined by the water vapor pressure, which is only a function of temperature. In contrast, the convective flow of hydrogen, oxygen and nitrogen all increase with increasing pressure. Increasing the pressure will allow high flow rates of the feed gases without altering the convective flow of water from the fuel cell!

#### 4.2. Plug flow reactor fuel cell

At the other limit of flow is when there is no diffusive mixing along the flow channels of the fuel cell, which is the equivalent of a plug flow reactor (PFR). In that case the diffusive term in Eq. (1) is zero. The right hand side of Eq. (1) must be greater than or equal to zero everywhere, in particular at the inlet of the flow channel. In plug flow there is no axial diffusion. If the water partial pressure were decreasing at the inlet (the right hand side of Eq. (1) being less than zero at the inlet,  $z = 0$ ) the inlet of the fuel cell would dry out and this would lead to a front moving from the inlet to the outlet, eventually drying out the entire fuel cell. The requirement for auto-humidification with the plug flow reactor is given by Eq. (6)

$$\begin{aligned} \left[ \frac{F_A^{\text{in}} + F_C^{\text{in}}}{A_{\text{channel}}} - \frac{j(z=0)}{4F} \right] \frac{P_w^o}{P_T} < \frac{j(z=0)}{2F}, \\ \left[ \frac{F_A^{\text{in}} + F_C^{\text{in}}}{A_{\text{channel}}} - \frac{j(P_w^{\text{in}})}{4F} \right] \frac{P_w^o}{P_T} < \frac{j(P_w^{\text{in}})}{2F} \end{aligned} \quad (6)$$

The current density at the inlet depends on the water activity at the inlet. Eq. (6) is the differential form of Eq. (2). The minimum current density to sustain auto-humidified operation in a PFR fuel cell is given by Eq. (7)

$$\left[ \frac{F_A^{\text{in}} + F_C^{\text{in}}}{A_{\text{channel}}} \right] < \frac{j(P_w^{\text{in}})}{4F} \left( 2 + \frac{P_w^o}{P_T} \right) \quad (7)$$

The difference between the auto-humidification requirements for a plug flow fuel cell and a stirred tank fuel cell reactor is that the current density must be self-sustaining at the inlet water vapor pressure, whereas the stirred tank must have a current density that is self-sustaining at the outlet water vapor pressure

$$\frac{\left[ \frac{F_A^{\text{in}} + F_C^{\text{in}}}{A_{\text{channel}}(2 + P_w^0/P_T)} \right]_{\text{PFR}}}{\left[ \frac{F_A^{\text{in}} + F_C^{\text{in}}}{A_{\text{channel}}(2 + P_w^0/P_T)} \right]_{\text{STR}}} = \frac{[j(P_w^{\text{in}})]_{\text{PFR}}}{[j(P_w^{\text{out}})]_{\text{STR}}} = \frac{[\rho(P_w^{\text{out}})]_{\text{STR}}}{[\rho(P_w^{\text{in}})]_{\text{PFR}}} \quad (8)$$

The current density scales inversely with the resistivity of the MEA. The pressure, temperature flow requirements for auto-humidified operation of a PFR fuel cell can be scaled to the requirement conditions for the STR fuel cell, with the scaling factor being the inverse ratio of the resistivity at the inlet and outlet water vapor pressures, as shown in Eq. (8). Because the membrane resistance at the low relative humidity of the feed is much greater than the membrane resistance at the high relative humidity of the effluent, the PFR fuel cell is more restricted in the ranges of temperature, pressure and flow rate where auto-humidification can be sustained.

From this analysis it is clear that a fuel cell with flow channels that resembles a PFR design will only function with auto-humidification at very limited conditions. The experiments showed that the serpentine flow channel fuel cell performed almost as well as the STR PEM fuel cell at the lower current densities. The effect of the flow channels was not as significant as Eq. (8) would suggest. The PFR model assumes no axial dispersion of water in the fuel cell, which is a worse case scenario. In the serpentine flow channel fuel cell there is axial dispersion due to concentration gradients in the flow channels. There is also water diffusion in the membrane both axially as well as laterally between adjacent flow channels. The dispersion of water by diffusion results in a fuel cell performance intermediate to the STR fuel cell and the PFR fuel cell.

#### 4.3. Consequences for fuel cell design

The key results for fuel cell design are contained in Eqs. (2) and (7). These equations present the relationship between current, feed flow rates, pressure and temperature required for auto-humidified operation of PEM fuel cells. Both experimental and analytic results demonstrate that auto-humidification is improved at higher pressures, lower flow rates and lower temperatures.

A second important result from the experiments and analysis is that fuel cells with long parallel flow channels are a poor design for auto-humidified operation. The open plenum type design of the STR fuel cell is superior because it promotes “back-mixing” of the water formed in the fuel cell with the feed to uniformly humidify the membrane-electrode-assembly.

A less obvious advantage of the STR design and the absence of flow channels is the reduction in flooding of water in the flow channels causing mass transfer limitations at high current densities. The STR PEM fuel cells could be operated to high current densities without observing any significant drop off in

the  $j$ - $v$  performance due to mass transport limitations; the mass transport limitations were seen for the serpentine flow channel fuel cells with both humidified and dry feeds. The mass transport limitations are due to water build-up in the flow channels restricting the oxygen and hydrogen from getting to the electrode/electrolyte interface. Without the flow channels the STR design permits the water to fall by gravity to the exit of the fuel cell; this self-draining feature provides for superior performance at lower flow rates which improves fuel utilization.

Flooding in PEM fuel cells has generally been thought to occur by water condensation in the gas diffusion layer [29–31]. In a recent paper we showed that the gas diffusion layer is hydrophobic which excludes liquid water from the GDL [21]. Liquid water only enters the GDL under a hydrostatic pressure sufficient to overcome the surface wetting force. The implication of a hydrophobic GDL is that liquid water will condense in the gas flow channels before it will condense in the gas diffusion layer, as illustrated schematically in Fig. 1. Liquid water will accumulate in the gas flow channels and hinder gas from entering the GDL, which will cause the mass transfer limitation. Because the carbon bipolar plate and the GDL are both hydrophobic water will bead off the surfaces if allowed to drain by gravity. By creating a free draining plenum as shown in Figs. 2 and 3 the liquid water drains off the surface of the GDL and does not create a significant mass transfer limitation. In contrast, the serpentine flow reactor requires a gas flow to push the liquid water droplets through the flow channels. The serpentine flow channels do not take advantage of gravity to drain the liquid water, and the result is a mass transfer limitation because of the liquid water accumulation in the flow channels. There was a recent paper by Li et al. using a pillared bipolar plate that achieved similar improvements in operation at high currents to what we present here [32]. The self-draining feature for liquid water depends critically on the orientation of the fuel cell. If we oriented the fuel cell shown in Figs. 2 and 3 in a horizontal configuration the flooding and mass transfer limitations become much worse!

The advantages of the STR over the PFR reactor design can be summarized as follows:

- i. Back-mixing: Back-mixing creates uniform concentration of reactants in an STR. The concentration of reactants and the RH (if the gas stream is not fully saturated) change along the length of the PFR flow channels. Concentration gradients cause current gradients [22]. Current gradients combine with RH gradients to cause changes in the water uptake of the membrane. When parts of the membrane become drier, the internal resistance increases and this area become hotter. These “hot spots” cause membrane failure.
- ii. Auto-humidification: Back-mixing allows the STR fuel cell to auto-humidify the entire anode and cathode reaction chambers [25]. A drop of water formed near the exit of the fuel cell permits water vapor to back diffuse toward the entrance.
- iii. Reduction in gas velocity: The gas velocity in PFR fuel cells is usually high to prevent blockages in the flow channels and flooding of the GDL. This is not necessary in a STR fuel cell as it can be orientated to self-drain.

- iv. Orientate to self-drain and enhance high current operability: By simplifying the reaction chamber design and removing the need for tortuous flow channels it is possible to orient the STR fuel cell to self-drain liquid water using gravity. PFR fuel cells are susceptible to blockage of the flow channels and flooding of the GDL.

#### 4.4. Systems implementation considerations

The STR concept lends itself well to a modular design concept. Current fuel cell systems are designed as one or two stacks of cells. To handle the current requirements the areas of the individual cells must be large (typically  $\sim 10^3 \text{ cm}^2$ ). To deliver the fuel across the cell the flow rates in the flow channels is very high at the inlet, this would clearly be problematic with dry feeds. In addition, if one cell fails, the entire stack is compromised [26]. Once a failure has occurred the whole stack needs to be removed. Additionally it is typical in this system for a single failure to cause failure in other related cells because the cells are coupled.

Modularity is our design solution to this problem, and the proposed STR fuel cell design lends itself extremely well to this concept for a number of reasons. The essence of our proposed design is that rather than rely on 1–2 large stacks the design would implement a series of smaller standardized modules which are self contained stacks and can be easily integrated into the system (similar to placing batteries into a radio for example). Instead of the 1–2 custom designed stacks, a series of standard (e.g. 1 kW) modules which are simply and easily combined and integrated into the system to get the desired power requirement would be employed (e.g. a stand alone stack with click in and click out connectors). This design has a number of significant advantages:

- (i) Cell failure no longer compromises the entire system.
- (ii) Design flexibility is enhanced in terms of sizing requirements and peak load requirements.
- (iii) Design flexibility is optimized specifically in terms of space utilization which is critical for automotive applications.
- (iv) Inter-changeability, maintenance and repairs are quicker, cheaper and simpler.
- (v) Parts are easier to acquire.
- (vi) Commercially there are many advantages of having one standardized product which can be simply scaled for many commercial applications.
- (vii) Improved efficiency for variable load.

## 5. Conclusions

Auto-humidified operation of PEM fuel cells up to temperatures of  $115^\circ\text{C}$  was demonstrated with a novel self-draining channel-less fuel cell. The design of this fuel cell was based on a reactor analysis of the fuel cell that indicated improved operation could be achieved by removing the flow channels. It was demonstrated that the PFR flow channel design prevalent in PEM fuel cells today may not be the optimal flow channel design.

An analysis of operating PEM fuel cells with dry feeds resulted in explicit criteria relating current density, feed flow rates, pressure and temperature required for auto-humidified operation. The STR fuel cell design was shown theoretically and experimentally to perform better than fuel cells with serpentine flow channels, and the STR fuel cell with dry feeds could even perform comparably to a serpentine flow channel fuel cell with humidified feeds.

The advantages of the dry feed, auto-humidified channel-less self-draining PEM fuel cell are:

- (i) There is no requirement to humidify feeds.
- (ii) Longer linear  $I$ – $V$  response of the cells due to reduced mass transport limitations.
- (iii) Back-mixing to remove fronts, concentration and current gradients.
- (iv) The ability to self-drain liquid water.

Additionally there are advantages for liquid feed fuel cells, specifically for portable applications, which reduce the need for pumps and balance of plant. Furthermore, a modular design concept utilizing the STR fuel cell design was introduced to increase the robustness of PEM fuel cell systems and make them more flexible for commercial applications. All this was achieved by applying simple chemical engineering design heuristics to the fuel cell design challenge.

## Acknowledgements

WH acknowledges funding from the Australian–American Fulbright Commission and the ARC Centre for Functional Nanomaterials. This work was supported in part by the NSF (DMR-0213707 and CTS-0354279).

## References

- [1] P. Grant, Hydrogen lifts off – with a heavy load, *Nature* 424 (2003) 129–130.
- [2] G. Konrad, M. Sommer, B. Loschko, A. Schell, A. Docter, *Handbook of Fuel Cells*, vol. 4, Wiley, Indianapolis, 2003, pp. 693–713.
- [3] H. Gasteiger, M. Mathias, Fundamental research and development challenges in polymer electrolyte fuel cell technology, in: *Materials for High Temperature PEM Fuel Cells*, The Energy Institute, Penn State University, USA, 2003.
- [4] W.H.J. Hogarth, J.C. Diniz da Costa, G.Q. Lu, Solid acid membranes for high temperature ( $>140^\circ\text{C}$ ) proton exchange membrane fuel cells, *J. Power Sources* 142 (1–2) (2005) 223–237.
- [5] O. Savadogo, Emerging membranes for electrochemical systems\*1. Part II. High temperature composite membranes for polymer electrolyte fuel cell (PEFC) applications, *J. Power Sources* 127 (1–2) (2004) 135–161.
- [6] T.M. Thampan, N.H. Jalani, P. Choi, R. Datta, Systematic approach to design higher temperature composite PEMs, *J. Electrochem. Soc.* 152 (2) (2005) A316–A325.
- [7] C. Yang, P. Costamagna, S. Srinivasan, J. Benziger, A.B. Bocarsly, Approaches and technical challenges to high temperature operation of proton exchange membrane fuel cells, *J. Power Sources* 103 (1) (2001) 1–9.
- [8] X.G. Li, M. Sabir, Review of bipolar plates in PEM fuel cells: flow-field designs, *Int. J. Hydrogen Energy* 30 (4) (2005) 359–371.
- [9] Z.G. Qi, A. Kaufman, PEM fuel cell stacks operated under dry-reactant conditions, *J. Power Sources* 109 (2) (2002) 469–476.
- [10] T. Van Nguyen, M.W. Knobbe, A liquid water management strategy for PEM fuel cell stacks, *J. Power Sources* 114 (1) (2003) 70–79.

- [11] N. Rajalakshmi, T.T. Jayanth, R. Thangamuthu, G. Sasikumar, P. Sridhar, K.S. Dhathathreyan, Water transport characteristics of polymer electrolyte membrane fuel cell, *Int. J. Hydrogen Energy* 29 (10) (2004) 1009–1014.
- [12] X.G. Yang, N. Burke, C.Y. Wang, K. Tajiri, K. Shinohara, Simultaneous measurements of species and current distributions in a PEFC under low-humidity operation, *J. Electrochem. Soc.* 152 (4) (2005) A759–A766.
- [13] M.V. Williams, H.R. Kunz, J.M. Fenton, Operation of Nafion((R))-based PEM fuel cells with no external humidification: influence of operating conditions and gas diffusion layers, *J. Power Sources* 135 (1–2) (2004) 122–134.
- [14] K.H. Choi, D.H. Peck, C.S. Kim, D.R. Shin, T.H. Lee, Water transport in polymer membranes for PEMFC, *J. Power Sources* 86 (1–2) (2000) 197–201.
- [15] G.J.M. Janssen, A phenomenological model of water transport in a proton exchange membrane fuel cell, *J. Electrochem. Soc.* 148 (12) (2001) A1313–A1323.
- [16] M. Ciureanu, M. Badita, Water balance experiments in PEM FC stacks. Measurements of water transport across the NAFION membrane, *J. New Mater. Electrochem. Syst.* 6 (3) (2003) 163–168.
- [17] J. Benziger, E. Chia, E. Karnas, J. Moxley, C. Teuscher, I.G. Kevrekidis, The stirred tank reactor polymer electrolyte membrane fuel cell, *AIChE J.* 50 (8) (2004) 1889–1900.
- [18] J. Benziger, E. Chia, J.F. Moxley, I.G. Kevrekidis, The dynamic response of PEM fuel cells to changes in load, *Chem. Eng. Sci.* 60 (6) (2005) 1743–1759.
- [19] E. Chia, J. Benziger, I.G. Kevrekidis, Water balance and multiplicity in a polymer electrolyte membrane fuel cell, *AIChE J.* 50 (9) (2004) 2320–2324.
- [20] J.F. Moxley, S. Tulyani, J.B. Benziger, Steady-state multiplicity in the auto-humidification polymer electrolyte membrane fuel cell, *Chem. Eng. Sci.* 58 (20) (2003) 4705–4708.
- [21] J. Benziger, J. Nehlsen, D. Blackwell, T. Brennan, J. Itescu, Water flow in the gas diffusion layer of PEM fuel cells, *J. Membr. Sci.* 261 (2005) 98–106.
- [22] A. Hakenjos, A. Muentert, U. Wittstadt, C. Hebling, A PEM fuel cell for combined measurement of current and temperature distribution and flow field flooding, *J. Power Sources* 131 (2004) 213–216.
- [23] W.H.J. Hogarth, R. Mejia-Ariza, E. Kimball, J.B. Benziger, Effect of gas composition on mass transfer to the cathode/membrane interface, *AIChE J.*, submitted for publication.
- [24] W.H.J. Hogarth, J.B. Benziger, Dynamic operation of a PEMFC: the presence of multiple steady states, *Electrochem. Solid State Lett.*, submitted for publication.
- [25] W.H.J. Hogarth, J.B. Benziger, Understanding the water balance in a PEMFC: removing the need for humidification, *J. Electrochem. Soc.*, submitted for publication.
- [26] J. Nehlsen, W.H.J. Hogarth, J. Benziger, Fuel cell design: the impact of PEM fuel cell dynamics on control and system design, *AIChE J.*, submitted for publication.
- [27] C.H. Woo, W.H.J. Hogarth, J. Benziger, PEM fuel cell current control by fuel starvation, *AIChE J.*, submitted for publication.
- [28] C. Yang, S. Srinivasan, A.B. Bocarsly, S. Tulyani, J.B. Benziger, A comparison of physical properties and fuel cell performance of Nafion and zirconium phosphate/Nafion composite membranes, *J. Membr. Sci.* 237 (1–2) (2004) 145–161.
- [29] U. Pasaogullari, C.Y. Wang, Liquid water transport in gas diffusion layer of polymer electrolyte fuel cells, *J. Electrochem. Soc.* 151 (3) (2004) A399–A406.
- [30] A.Z. Weber, J. Newman, Modeling transport in polymer–electrolyte fuel cells, *Chem. Rev.* 104 (2004) 4679–4726.
- [31] C.Y. Wang, Fundamental models for fuel cell engineering, *Chem. Rev.* 104 (2004) 4727–4766.
- [32] P.W. Li, S.P. Chen, M.K. Chyu, Novel gas distributors and optimization for high power density in fuel cells, *J. Power Sources* 140 (2005) 311–318.